CONTROL SCHEME EVALUATION FOR CLASS-D AMPLIFIERS IN A POWER-ULTRASONIC SYSTEM

Y.Wang, M.J.Draper †, S.M.Denley †, F.V.P.Robinson*, P.R.Shepherd**

**University of Bath, United Kingdom, yw244@bath.ac.uk*
†Sonic Systems Ltd, United Kingdom, info@sonicsystems.co.uk

Keywords: Power-Ultrasonics, Piezoelectric-transducer, Class-D, PPWM, PSPICE.

Abstract

Power-converters or amplifiers are required to drive high-power piezoelectric transducers and attached processing equipment, at the optimum resonance mode for best processing efficacy, while under varying loading conditions. The driving power converter must synthesize relatively low-distortion sinusoidal output current to prevent harmonic-current excitation of neighbouring, less-productive or desirable resonant modes. Continuously-variable output-voltage capability is required to maintain output power at a level which optimises processing. Three output synthesis methods have been reviewed in this paper for the Class-D amplifier constituting the transducer driver. Typical output-waveform quality is assessed, and PSPICE simulation and laboratory results are presented to illustrate performance.

1 Introduction

Power-ultrasonic transducers of up to several kilowatts are being increasingly applied in food processing and chemical and material handling equipment, to accelerate chemical reactions, and improve material dispersion, mixing, sieving etc. Such systems use one, or a number of, piezoelectric transducers to excite vibration at one of the natural resonant modes of the transducer(s), usually, when attached to the processing equipment, and to track the changing resonant-frequency under different operating conditions. This minimizes the acoustic power that must be coupled to maintain the required optimum vibration level. Typical operating frequencies range from 20 to 120kHz [19].

A typical power-ultrasonic system comprises the ultrasonic transducer and its power generator, as shown in Fig.1. The generator is usually mains-supply powered and delivers an approximately sinusoidal output current to one or more transducers. Such a generator usually contains automatic frequency- and amplitude-setting control loops, which ensure that the ultrasonic power to the acoustic load is generated at the desired level and correct resonant frequency for the processing equipment and material involved [9,10,23].

A number of power-converter control options have been identified and analyzed, including quasi-squarewave (QS) operation and sine-wave pulse-width-modulation (PWM) and programmed PWM (PPWM) operation, as part of this work to design and develop an efficient, easily controlled generator system with a power-factor-corrected input stage for direct-off-line mains-supply connection.

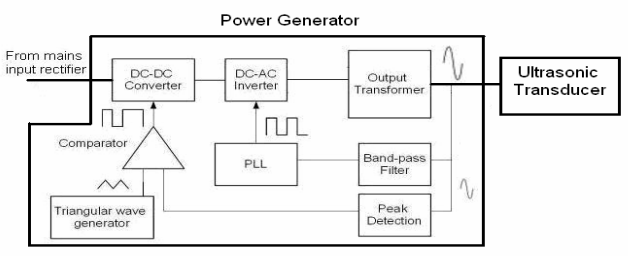

Figure.1 Two main control loops of existing power converter.

2 Existing Control Loops

Fig.1 shows the two main control loops which are typically found in an existing power-ultrasonic system, namely, current feedback loop and frequency control loop [1,21]. The DC-DC converter draws its input via a mains rectifier and its output level is regulated to satisfy the load power required. Its output is fed to the DC-AC inverter which operates at the load resonant frequency. The load resonant-frequency changes with operating conditions and is tracked by a phase lock loop (PLL) [9,10,14,15,18,20]. The load current is sensed in the secondary winding of the output transformer and is used for both current and frequency control.

Using two separate power converters for amplitude and frequency control results in greater conversion losses, component count and system volume than a single-stage inverter topology, which enables both amplitude and frequency control. To implement a single-stage alternative, three output-waveform synthesis methods have been considered.

3 Output waveform synthesis methods

3.1 Quasi-squarewave

When QS control is used with the H-bridge topology shown in Fig.2[2], the drive and output waveform patterns are as illustrated in Fig.3[23]. Both the pulse width and period of the waveform can be varied to satisfy the instantaneous power required and resonant frequency, respectively. As a result a constant bus voltage can be used in this case.

Fourier analysis allows the variation of the fundamental and harmonic amplitudes of V_{AB}, to be predicted as half-bridge switching delay, T_d, is increased; see in Equations (1) and (2). To do this, the time axis is changed to a radian-angle axis as

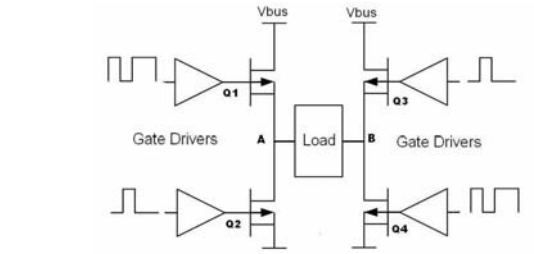

Figure.2 H-bridge topology with four gate drivers.

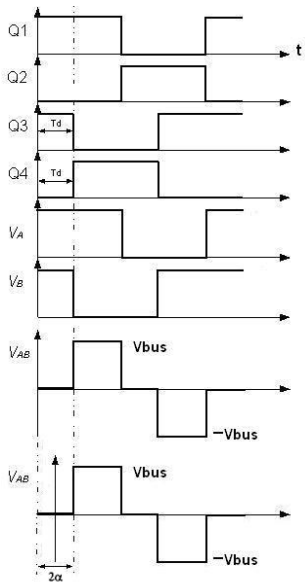

Figure.3 Typical waveforms for QS operation.

shown in Fig.3, with the time-zero adjusted to make V_{AB} have odd, quarter-wave symmetry, to give odd, sine harmonic content only. The delay T_d is represented by 2α, where α is the switching angle. The output waveform must not contain DC content and must have a zero average value. The magnitudes of the fundamental and harmonic components are derived using Equation (1).

$$V_h = \frac{1}{\pi}\int_0^{2\pi} V_{AB}(\omega t)\sin(h\omega t)\,d\omega t \qquad (1)$$

where h=1,3,5… and is the harmonic order.

When the switching delay angle is expressed in terms of α, and amplitude in terms of V_{BUS} the DC bus voltage in Equation (1) may be reduced to Equation (2).

$$V_h = \frac{4V_{BUS}}{h\pi}\cos(h\alpha) \qquad (2)$$

Therefore, the fundamental-component amplitude varies with α as in (3). Its value decreases from 1, when α is 0°, to 0 when α is 90° [7].

$$V_1 = \frac{4V_{BUS}}{\pi}\cos(\alpha) \qquad (3)$$

Fig.4 shows the normalized amplitude of the first three output voltage harmonics when QS is used as the control method. Despite the attraction of simplicity, its output voltage contains high levels of low-order harmonics and therefore is very likely to excite at the undesired higher-frequency resonant modes without additional sophisticated filtering circuits.

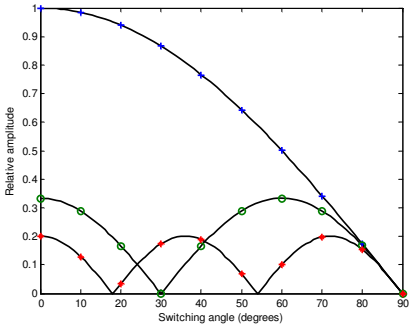

Figure.4 Normalized amplitudes of fundamental '+', 3rd harmonic 'o' and 5th harmonic '*'.

3.2 Sinewave-PWM

The second possible approach is to implement PWM of higher switching frequencies in order to generate a purer sinewave load current with reduced low-order harmonics [16]. Again using the full H-bridge circuit in Fig.2, Fig.5 shows typical circuit waveforms for a sinewave-weighted PWM switching scheme with 10 pulses per base-band period.

However, since a typical ultrasonic system operates from 20 to 120kHz, a 10-pulse scheme would require an excessively high switching frequency, i.e. greater than 1MHz, which would increase switching loss unacceptably and lower system efficiency. Therefore only PWM control with up to 5 pulses will be considered.

Modulation index, m_a, is the amount of full-scale signal that can be output from the PWM amplifier. It is given in Equation (4) as the amplitude ratio of the input signal V_{IN} to the carrier signal V_C [8]:

$$m_a = \frac{V_{IN}}{V_C} \qquad (4)$$

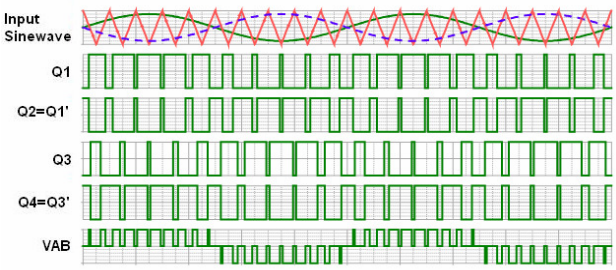

Figure.5 Typical waveforms for PWM with 10 pulses

3.3 Programmed-PWM

The concept of PPWM was first introduced in 1973 as a scheme to perform effective harmonic elimination by

inserting an even number of symmetric zero-voltage gaps into each positive and negative section of the squarewave [6,17]. Fig.6 shows a PPWM waveform with 2 and 4 gaps inserted (number of switching angles $N = 3, 5$) in each half waveform.

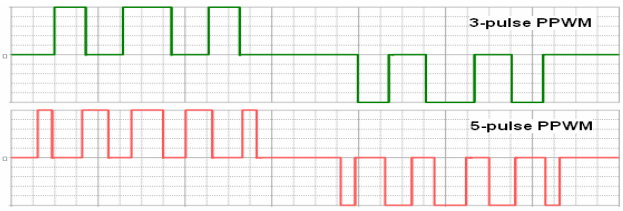

Figure.6 3- and 5-pulse PPWM waveform v_{PPWM}.

Using Fourier analysis, the PPWM waveform of unit amplitude can be shown as:

$$v_{PPWM}(\omega t) = \sum_{h=1}^{\infty} [a_h \sin(h\omega t) + b_h \cos(h\omega t)] \qquad (5)$$

Due to the odd, quarter-wave symmetry in Fig.7, the Fourier coefficients are given by:

$$\begin{cases} a_h = \dfrac{4}{h\pi}\sum_{k=1}^{N}(-1)^{k+1}\cos(h\alpha_k) & h-odd \\ a_h = 0 & h-even \\ b_h = 0 & h = 1,2,\cdots N \end{cases} \qquad (6)$$

where switching angles $0 < \alpha_1 < \alpha_2 < \ldots\ldots < \alpha_N < \dfrac{\pi}{2}$. The magnitude of the fundamental and harmonic components can be calculated by:

$$V_h = \frac{4}{h\pi}\sum_{k=1}^{N}(-1)^{k+1}\cos(h\alpha_k)$$

where

$$\begin{cases} V_1 = \dfrac{4}{\pi}\sum_{k=1}^{N}(-1)^{k+1}\cos(\alpha_k) = m_a \\ V_3 = \dfrac{4}{3\pi}\sum_{k=1}^{N}(-1)^{k+1}\cos(3\alpha_k) = 0 \\ \vdots \\ V_{2N-1} = \dfrac{4}{(2N-1)\pi}\sum_{k=1}^{N}(-1)^{k+1}\cos((2N-1)\alpha_k) = 0 \end{cases} \qquad (7)$$

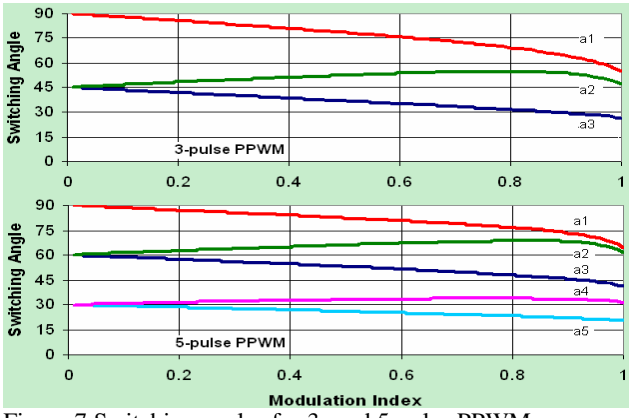

Figure.7 Switching angles for 3- and 5-pules PPWM.

Equation (7) implies that if the PPWM switching pattern is designed to eliminate 3rd, 5th … $(2N\text{-}1)^{th}$-order harmonics, N equations and N variables, $\alpha_1 \ldots \alpha_N$, need to be solved [3,5,12]. For example, the required switching angles for PPWM of $N = 3$ to eliminate the 3rd and 5th-order as well as $N = 5$ to eliminate the 3rd, 5th, 7th and 9th-order harmonics, to allow the modulation index, m_a, to be varied from 0 to 1, have been previously computed and are shown in Fig.7 .

4 Simulation using SPICE

4.1 Piezoelectric transducer modelling

To compare and assess power-converter performance, and help identify and understand the effects of load impedance characteristics, a PSpice model has been developed for an existing sandwiched, 35kHz transducer [4] as shown in Fig.8. Transmission lines *T_BACK*, *T_CERAMIC*, *T_FRONT* and *T_BOLT* represent the transducer back mass, piezoelectric ceramics, front mass and bolt respectively. C_1 and C_2 are measured and calculated based on the transducer static capacitance. *EGND* and *MGND* are electrical and mechanical grounds respectively. Detailed information on the structure and parameter calculations of PSpice transducer model using transmission line and controlled source is beyond the scope of this paper but can be found in [11,13].

Fig.9 compares admittance and resonant frequencies in simulation and real measurements. These two sets of measurements agree relatively well in terms of admittance values and variation with frequency. The 0.3kHz difference in resonant frequencies, less than 1%, may arise due to the approximation of transducer physical dimensions, e.g. layers of front masses, which vary in size, and have been simplified to one transmission line model with constant diameter and acoustic velocity.

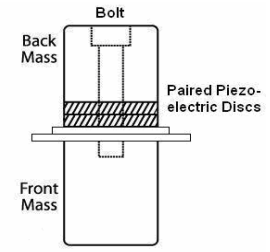

(a)

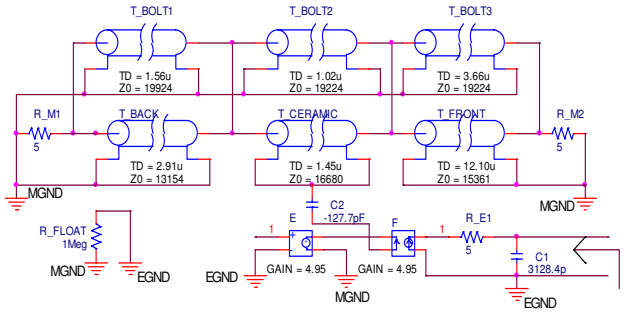

(b)

Figure.8 (a) Structure of a 35kHz Ultrasonic transducer; (b) PSpice transmission-line model of (a).

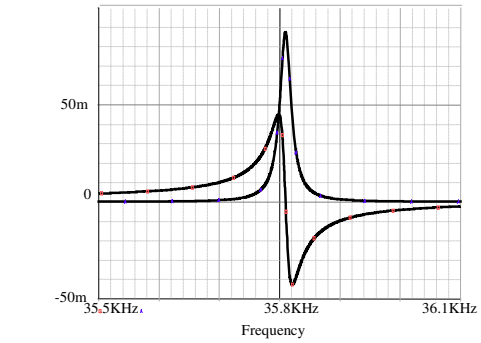

(a)

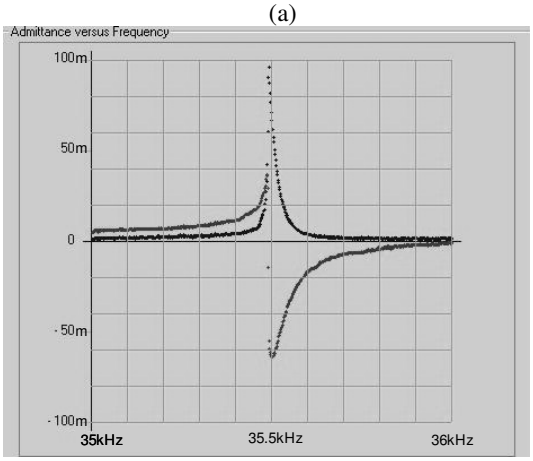

(b)

Figure.9 Real and imaginary part of transducer admittance plots of desired resonant mode around 35kHz: (a) PSpice simulation; (b) real measurement as in [23].

4.2 Switching simulation with matching inductor

Fig. 10 shows the simulation circuits for evaluating the performance of different control options. *L_MATCHING* is the matching inductor whose value is calculated as suggested in [22]. The two voltage controlled voltage sources *E*, model the function of the H-bridge inverter. The gain is chosen to be 100, representing a 100V DC bus voltage since the input PWM signal ranges from 0 to 1.

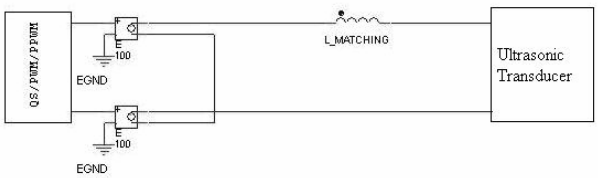

Figure.10 Simulation circuit for switching scheme evaluation.

4.3 Results and conclusions

First, the performance of harmonic elimination by delivering 80% of the full-scale output power, m_a =0.8, using different switching schemes is compared. Fig.11 shows the Fast Fourier Transform (FFT) of output voltages and load current. It can be seen that when N = 3, PPWM option eliminates 3rd and 5th harmonics and 5-pulse PPWM contains no harmonics up to the 9th order. However both QS and PWM shows the existence of these lower-order harmonics.

Normalized amplitudes of fundamental, 3rd, 5th and 7th harmonic currents given in Fig.12 show same performances over the linear modulation range for PWM and PPWM in accordance to Fig.11. Both PWM and PPWM give linear modulation when m_a is from 0 to 1. In order to eliminate up to the 5th harmonics, 5 pulses are required for PWM whilst with PPWM, pulse number is decreased to 3. Using fewer pulses results in lower switching losses therefore PPWM is considered as a more effective and efficient method compared with the other two options.

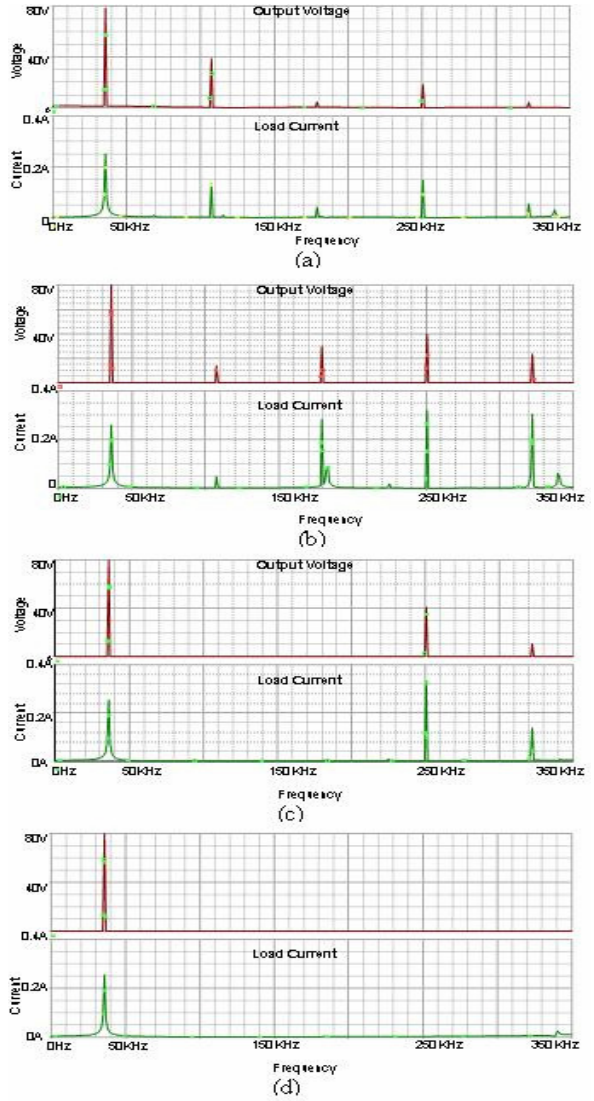

Figure.11 FFT of output voltage and load current with different switching schemes when delivering 80% of the full power capacity (a) QS; (b) N = 3 PWM; (c) N = 3 PPWM; (d) N = 5.

Fig.12 also indicates that no matter what scheme is applied, the more voltage pulses the better, since the current waveform will better approximate a sinewave. However, as expected PPWM is significantly better at reducing the 3rd harmonic

content which is likely to be most troublesome in exciting undesired resonant modes. PPWM, therefore, seems the best method to give an acceptable compromise between output-current harmonic distortion and power-semiconductor switching loss.

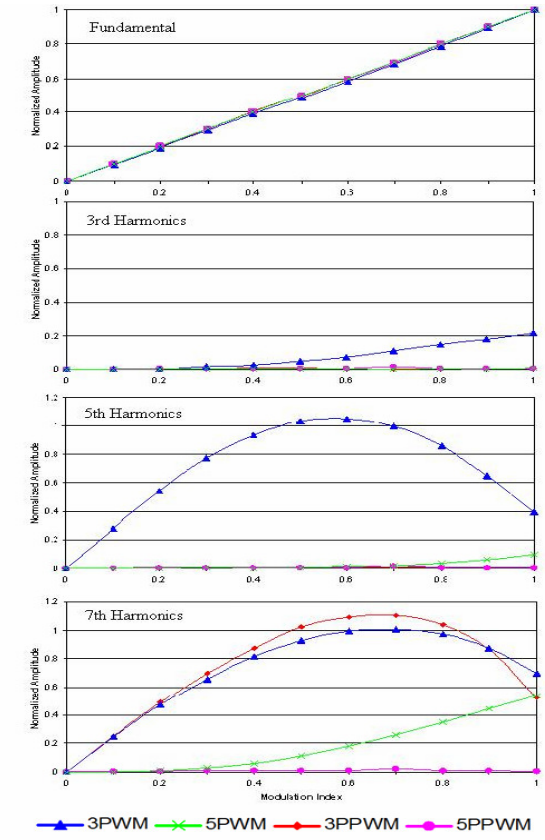

Figure.12 Normalized amplitude of fundamental and harmonics.

5 Measurements

In addition to the simulation in Section 4, laboratory experiments were also conducted to further prove the advantage of using PPWM in a typical power-ultrasonic system. Fig.13 shows a simplified diagram of testing environment. A Xilinx Spartan3E FPGA is programmed to form a self-contained PPWM waveform generator. Two isolated power-MOSFET drivers are used to drive the MOSFETs in the H-bridge topology. The bus voltage is set to be 50V and all DC voltages including 5V and 15V are supplied from a laboratory power supply.

Fig. 14 and 15 show experimental H-bridge voltage and current waveforms and their respective frequency spectra, which are in good agreement with simulation results.

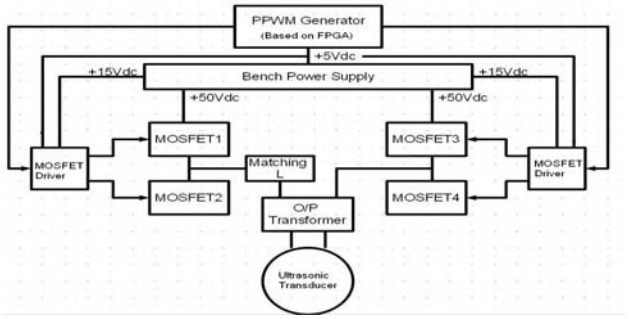

Figure.13 PPWM lab experiment test circuit diagram.

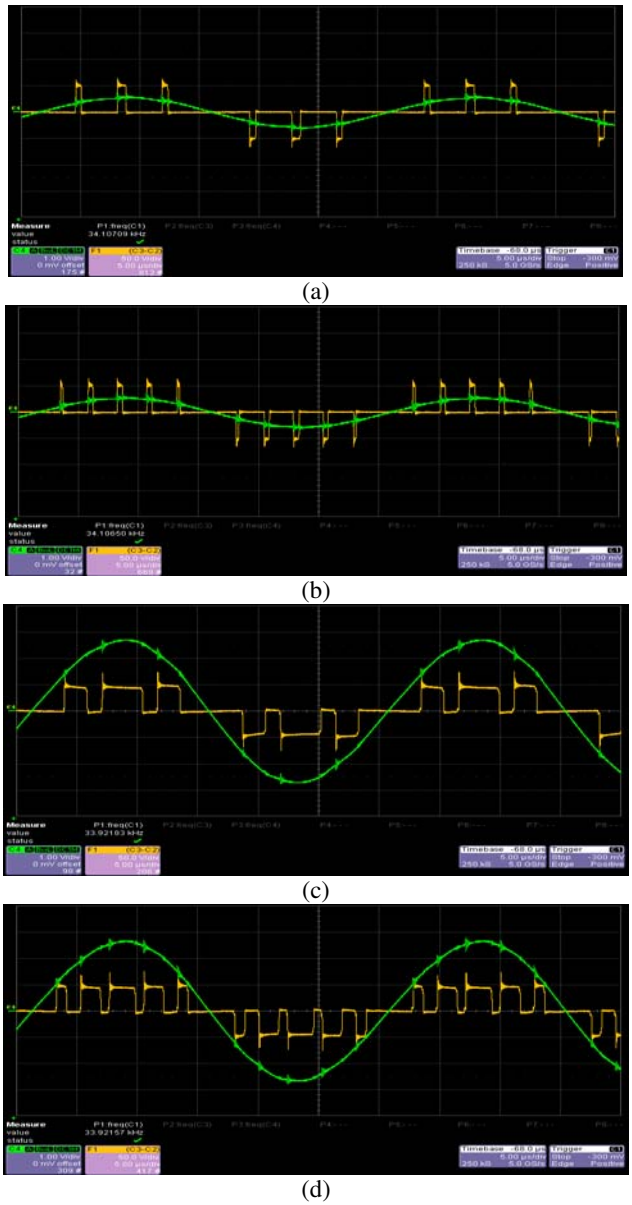

(a) (b) (c) (d)

Figure.14 Output voltage (F1) and load current (C4) when output power is (a) 10W with 3PPWM; (b) 10W with 5PPWM; (c) 100W with 3PPWM; (d) 100W with 5PPWM.

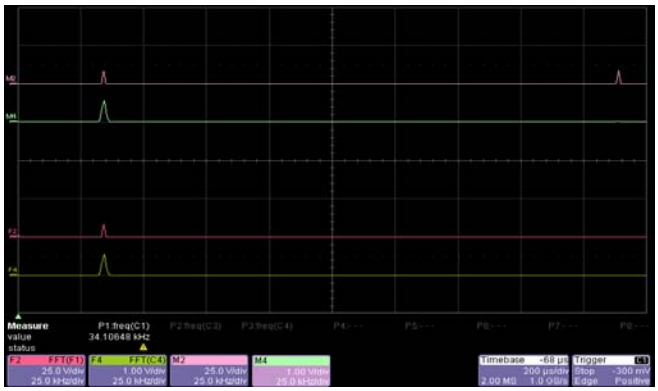

(a)

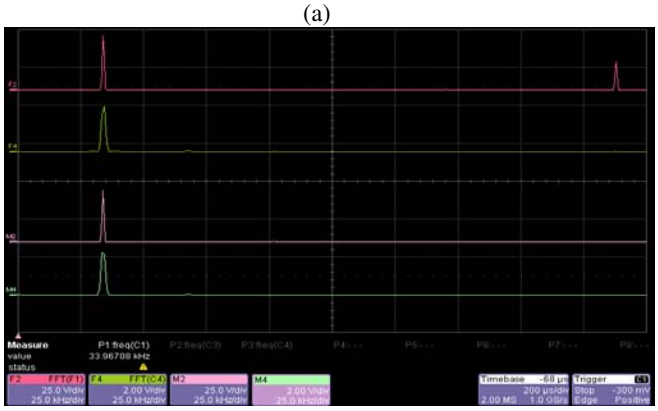

(b)

Figure.15 (a) FFT of Fig.14 (from top) M2-3PPWM output voltage,M4-3PPWM load current,F2-5PPWM output voltage, F4-5PPWM load current; (b) FFT of Fig.15 (from top): F2-3PPWM output voltage, F4-3PPWM load current, M2-5PPWM output voltage, M4-5PPWM load current.

6 Conclusions

Three possible variable-frequency variable-voltage waveform sysnthesis methods, including QS, PWM and PPWM, have been identified and investigated in this paper for application in power-ultrasonic-transducer drive amplifiers, or power-converters. Preliminary PSpice simulations and experimental validations have been conducted. Initial results show that PPWM waveform synthesis seems to give the best performance compromise in terms of balancing effective harmonic elimination and low switching loss.

References

[1] S. Ben-yaakov, E. Rozanov, T. Wasserman, T. Rafaeli, L. Shiv and G. Ivensky. "A resonant driver for a piezoelectric motor with single transistor direction switches", *15th Annual IEEE Applied Power Electronics Conference and Exposition,* vol.2, pp.1037-1043, (2000).

[2] J. S. Chang, M. T. Tan, Z. Cheng and Y. C. Tong. "Analysis and design of power efficient class d amplifier output stage", *IEEE Trans on Circuit and Systems I: Fundamental Theory and Applications*, vol.47(6), pp. 897-902, (2000).

[3] J. W. Chen and T. J. Liang. "A novel algorithm in solving nonlinear equation for programmed PWM inverter to eliminate harmonics", *23rd Annual Conference of IEEE Industrial Electronics Society (IECON 97),* vol.2, pp.698-703, (1997).

[4] J. Deventer, T. Lofqvist and J. Delsing. "PSpice Simulation of Ultrasonic Systems", *IEEE Transactions on Ultrasonics*, vol.47 (4), pp.1014-1024, (2000).

[5] P. N. Enjeti and J. F. Lindsay. "Solving nonlinear equations of harmonic elimination PWM in power control", *IEEE Electronics Letters*, vol.23(12),pp.656-657, (1987).

[6] P. N. Enjeti, P. D. Ziogas and J. F. Lindsay. "Programmed PWM techniques to eliminate harmonics: a critical evaluation", *IEEE Transactions on Industry Application*, vol.26 (2), pp.302-316, (1990).

[7] D. A. Grant, J. A. Houldwirth, and K. N. Lower. "A New High-Quality PWM AC Drive", *IEEE Transactions on Industry Applications*, vol.19 (2), pp. 211-216, (1983).

[8] D. G. Holmes and T. A Lipo. *Pulse Width Modulation for Power Converters: Principles and Practice*. Wiley-IEEE Press, (2003).

[9] J. Ishikawa, Y. Mizutani, T. Suzuki, H. Ikeda and H. Yoshida, "High-frequency drive-power and frequency control for ultrasonic transducer operating at 3MHz," *IEEE Industry Applications Conference Thirty-Second IAS Annual Meeting*, vol. 2, pp. 900-905, (1997).

[10] V. N. Khmelev, R. V. Barsokov, S. N. Tsyganok, and M.V. Khmelev "Phase lock system of ultrasonic electronic generators", *7th International Siberian Workshop and Tutorials EDM, (Session VI),* pp. 229-231, (2006).

[11] W. M. Leach, Jr. "Controlled-source analogous circuits and SPICE models for piezoelectric transducers", *IEEE Trans. Ultrason., Ferroelect., Freq. Contr.*, vol.41, pp. 60–66, (1994).

[12] L. Li, D. Czarkowski, Y. Liu and P. Pillay. "Multilevel selective harmonic elimination PWM technique in series-connected voltage inverters", *IEEE Transactions on Industry Applications*, vol.36 (1), pp.160-170, (2000).

[13] E. Maione, P. Tortoli, G. Lypacewicz, A. Nowicki and J. M. Reid. "PSpice modeling of ultrasound transducers: comparison of software models to experiment", *IEEE Trans. Ultrason., Ferroelect. Freq. Contr.*, vol.46, no.2, (1999).

[14] Y. Mizutani, T. Suzuki, H. Ikeda and H. Yoshida. "Automatic frequency control for maximizing RF power fed to ultrasonic transducer operating at 1 MHz", *1996 IEEE Industry Applications Conference Thirty-First IAS Annual Meeting*, vol.3, pp. 1585-1588, (1996).

[15] B. Mortimer, T. Du Bruyn, J. Davies and J. Tapson. "High power resonant tracking amplifier using admittance locking",*Ultrasonics*,vol.39(4),pp.257-261, (2001).

[16] N. Mohan, T. M. Undeland and W. P. Robbins. *Power Electronics: Converters, Applications and Design.* 3rd ed. Hoboken: Wiley, (2003).

[17] H. S. Patel and R. G. Hoft. "Generalized techniques of harmonic elimination and voltage control in thyristor inverter: part I- harmonic elimination", *IEEE Trans. on Industrial Application*, IA-9(3), pp.310-317, (1973).

[18] Y. Peng, J. Xu, and Y. Li. "Modeling and simulation of an improved PLL-controlled circuit for series resonant inverter", *International Conference on Electrical Machines and Systems*, pp. 1786-1788, (2008).

[19] J. P. Perkins. "An outline of power ultrasonics," *OEM Design*, London: Mercury House, (1972).

[20] L. J. Smith. "Use of phase-locked-loop control for driving ultrasonic transducer", *NASA Technical Note*, D-3567, (1966).

[21] L. Svilainis and G. Motiejunas. "Power amplifier for ultrasonic transducer excitation", *ULTRAGASRSAS*, Vol. 58(1), pp.30-36, (2006).

[22] C. M. Van Der Burgt and H. S. J. Pijls, "Motional positive feedback systems for ultrasonic power generators", *IEEE Transactions on Ultrasonics Engineering,* vol.10(1), pp.2-19, (1963).

[23] Y. Wang, M. Draper, S. Denley, F. Robinson and P. Shepherd, "Power converters for power-ultrasonic transducers", *46th International Universities' Power Engineering Conference,* section: power conversion, paper no. 203, (2011).